A prediction model for chloride-ion ingress in concrete sleepers

Morteza Esmaeili, Sadegh Kaviani, and Farzad Farivar

- Early deterioration and failure of prestressed concrete sleepers (crossties) is a common problem for railways in desert environments.
- This study tested concrete samples from B70 concrete sleepers in desert areas obtained from the field and from sleepers with early-stage deterioration transported from the field to the laboratory and representative cubic concrete samples to determine chloride contents and chloride diffusion rates.
- A proposed model for chloride diffusion in concrete sleepers subjected to desert environments was developed and validated using maintenance records.
- Analysis of the factors influencing chloride diffusion indicated that increasing concrete cover and adjusting mixture proportions to decrease the diffusion coefficient would be an effective way to increase the durability of concrete sleepers in desert environments.

Reportedly, about 30 million ha (74 million acres) of Iran's land area are classified as entirely desert areas, of which about 12 million ha (30 million acres) are exposed to windblown sand and about 5 million ha (12 million acres) are active sand dunes.[1] Zakeri et al. listed railway superstructure problems in the sandy desert areas, which are summarized as follows:

- breakage and wear of concrete, steel, and wooden sleepers (**Fig. A.1**; for appendix figures go to www.pci.org/2023Jan-Appx1)
- untimely wear of rails and fastening systems
- quick deterioration of track geometry
- gradual degradation of bridges
- obstruction of culvert entrances (**Fig. A.1**)
- structural damage due to excessive rigidity of ballast layer (**Fig. A.2**)
- track closure due to deposition of sand (**Figure A.2**)[2]

The B70 concrete sleeper is a monoblock sleeper designed by a factory in Germany. The compression test of cubic samples from these concrete sleepers should be at least 65 MPa (9.4 ksi). The prestressing reinforcement within these elements is provided by 7 mm (0.3 in.) diameter ST160 wires,

which are basically equivalent to ASTM A472, A416, and A421 material with a yield strength of 1400 MPa (200 ksi) and ultimate strength of 1800 MPa (260 ksi).[3] The geometry of the B70 concrete sleeper is optimized to performing best in the vertical and lateral directions; however, due to the thin concrete cover in parts of this sleeper, the prestressing wires are prone to deterioration in harsh environmental conditions.[3] According to the category of sleeper damages,[4] one challenge to railway structures is the chemical conditions of desert areas.[2,5] Some of the biggest obstacles to railway lines in desert areas are early cracking and deterioration of concrete sleepers, which cause tremendous maintenance costs.[6,7] Cracking and rapid deterioration of concrete sleepers in sandy blocks of the Iranian railway network have been reported less than five years after the commencement of service on these lines; however, concrete crossties should provide more than 50 years of service life.[8]

Numerous investigations have been done to predict the service life of concrete structures in marine areas, and several models have been proposed to estimate chloride diffusion and predict the time of corrosion initiation in such structures. Examples of these service life models include DuraPGulf, developed by the University of Tehran based on Persian Gulf data,[9] and Life 365, published by a consortium including the Slag Cement Association, the Concrete Corrosion Inhibitors Association, the National Ready Mixed Concrete Association, and the Silica Fume Association.[10] The neural network approach is also used as a subset of artificial intelligence applications in deterministic equations for service life models developed by the Concrete Technology and Durability Research Center (CTDRC) and the Building and Housing Research Center (BHRC).[11] The International Federation for Structural Concrete (*fib*) proposed the *fib* model based on research by DuraCrete and DARTS projects[12] and modified in 2012 by Ramazanipour et al. based on Persian Gulf information.[13] The DuraCrete model and the chloride diffusion model proposed by Van der Wegen et al. (CHLODIF) were also the first models developed to predict concrete service life and corrosion initiation of wires.[14,15]

However, few studies have been conducted on the deterioration of concrete sleepers in desert areas. In 2010, Mohammadzadeh and Vahabi investigated the effect of chloride ion ingress on the B70 concrete sleeper reliability index.[16] In that study, the ingress of chloride ions in Iran's desert conditions was attributed to corrosion of the steel wires, and the middle section of the sleeper showed higher vulnerability than other sections. Furthermore, increasing the height of the middle section of the concrete sleeper was proposed as the best solution to improve the reliability index of the sleeper. In 2016, Tadayon researched the causes of the failure of concrete sleepers in the desert regions of Iran.[17] In Tadayon's study, the following tests were performed to find the reasons for cracking:

- carbonation depth
- compressive strength of concrete cores
- volumetric electrical resistance
- electrical conductivity
- water absorption
- density, absorption, and voids in hardened concrete
- electrical conductance of concrete as an indication of the ability to resist chloride ion penetration
- amount of sulfur trioxide (SO_3) in concrete
- water-soluble chlorides in mortar and concrete
- petrography of concrete

The most important outcome of the study was that for sleepers in good condition with no preexisting cracks during construction and installation, no evidence of ettringite or other chemical reactions was observed except corrosion and swelling of reinforcing bars due to a significant amount of chloride ions in the concrete. Accordingly, Tadayon concluded that the cracking of concrete sleepers in these areas is a result of the corrosion of prestressed steel wires. Moreover, the combination of dynamic loading generated by passing traffic and the corrosion of steel wires due to chloride-ion ingress is considered the cause of early deterioration of the studied concrete sleepers.

Although studies have been conducted about prediction models for different structures, there is still a research gap with few studies about chloride diffusion and its rate in prestressed concrete sleepers in the desert environment, as well as the initiation of corrosion and the influential factors. Accordingly, the present study's main objective is to model chloride diffusion in prestressed concrete sleepers and investigate the influencing factors. Therefore, to obtain the required factors for the diffusion model, chloride profiles were obtained from field and laboratory experiments of cracked concrete sleepers exposed to sandy desert conditions in Iran. A model was developed based on the factors obtained from the experiments. Finally, the onset of corrosion was predicted and a sensitivity analysis of each of the influencing factors was performed. The results of this investigation and the proposed experimental model can be used to change concrete sleeper design and increase concrete sleepers' service life in severe conditions.

Field survey and condition assessment in desert areas

Another challenge associated with construction in drylands is the relatively shallow water table, which is drawn toward the surface either naturally or artificially. The potential for corrosion in concrete sleepers increases when water levels rise above the track structure bringing salt and water to the surface through capillary action and evaporation in hot deserts.[18,19]

A railway route through a closed plain in the Lut Desert was chosen for the field survey and concrete sleeper condition assessment in this study. Water flows into the plain from the surrounding mountains with no way out; thus, the groundwater level in the whole region, especially around the seasonal Shur-e Gaz River, is high, which is confirmed by the presence of scattered vegetation. Moreover, the railway route passes through the watershed of the Shur-e Gaz River. After water is drawn to the surface by the process of capillary action, the soil salinity increases because evaporation leaves salt on the surface layer of the soil. By this means, all the necessary conditions—saline soil, moisture, and oxygen—are available to create corrosion.

Windblown sands create many problems for railway lines, so it is useful to identify the affected sections of the railway network. The Islamic Republic of Iran Railways (RAI) categorizes the severity of sand in each area as low, medium, severe, and critical (**Fig. 1**).

Concrete sleepers have been used in approximately 8925 km (5546 mi), or 85%, of Iran's rail network, and in some areas with critical windblown sand conditions, concrete sleepers have experienced early cracking and failures.[20] In the surveyed blocks, the intensity of deposition of windblown sand leads to 24-hour repair and maintenance, and maintenance operations are in progress to replace broken concrete sleepers. Prestressed concrete B70 sleepers are used on these railway lines. **Figure 2** shows the plan view, side view, and cross sections of a B70 concrete sleeper.

Field inspections indicated that the failure pattern in these sleepers was typically the same (**Fig. A.3**). Failures often emerged as longitudinal cracks on the sleeper's two lateral surfaces and near the prestressed wire.

Observations from the field survey suggested that cracking and ultimate failure of concrete sleepers in the studied areas were due to corrosion and deterioration of the prestressed wires. Observations indicated that the prestressed reinforcement has severe corrosion and has lost cross-sectional area due to corrosion.

Field evaluation indicated that the cracking and deterioration of concrete sleepers followed a similar trend. Because the orientation and position of the cracks are similar, the deterioration process cannot be categorized by type of cracking.

The following three steps describe the deterioration process in these concrete sleepers.

Formation of longitudinal cracks in sleeper midspan adjacent to upper layer of wires

The appearance of longitudinal cracks in lateral surfaces is the first stage of the deterioration of the concrete sleepers.[16] The cracks, which often form in the center of the sleeper and near the top layer of reinforcing steel, progressively extend to both ends of the sleeper (**Fig. A.4**).

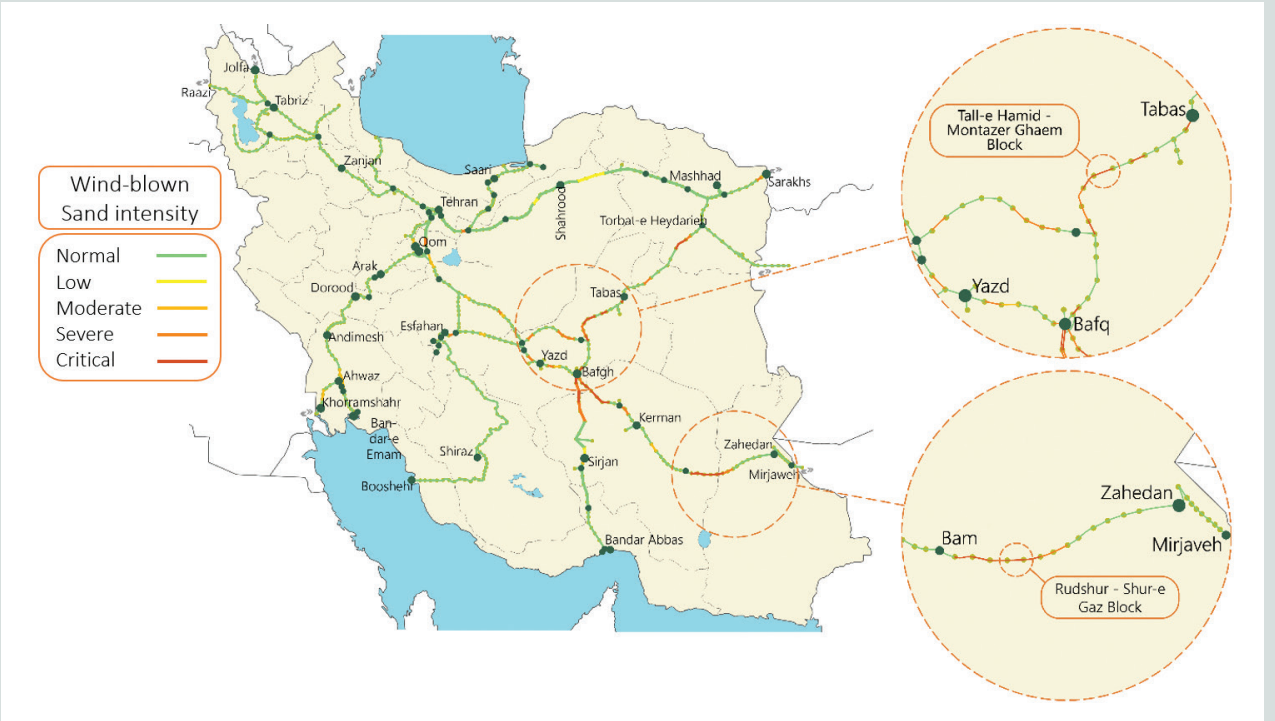

Figure 1. Windblown sand severity in Iran's railway network.

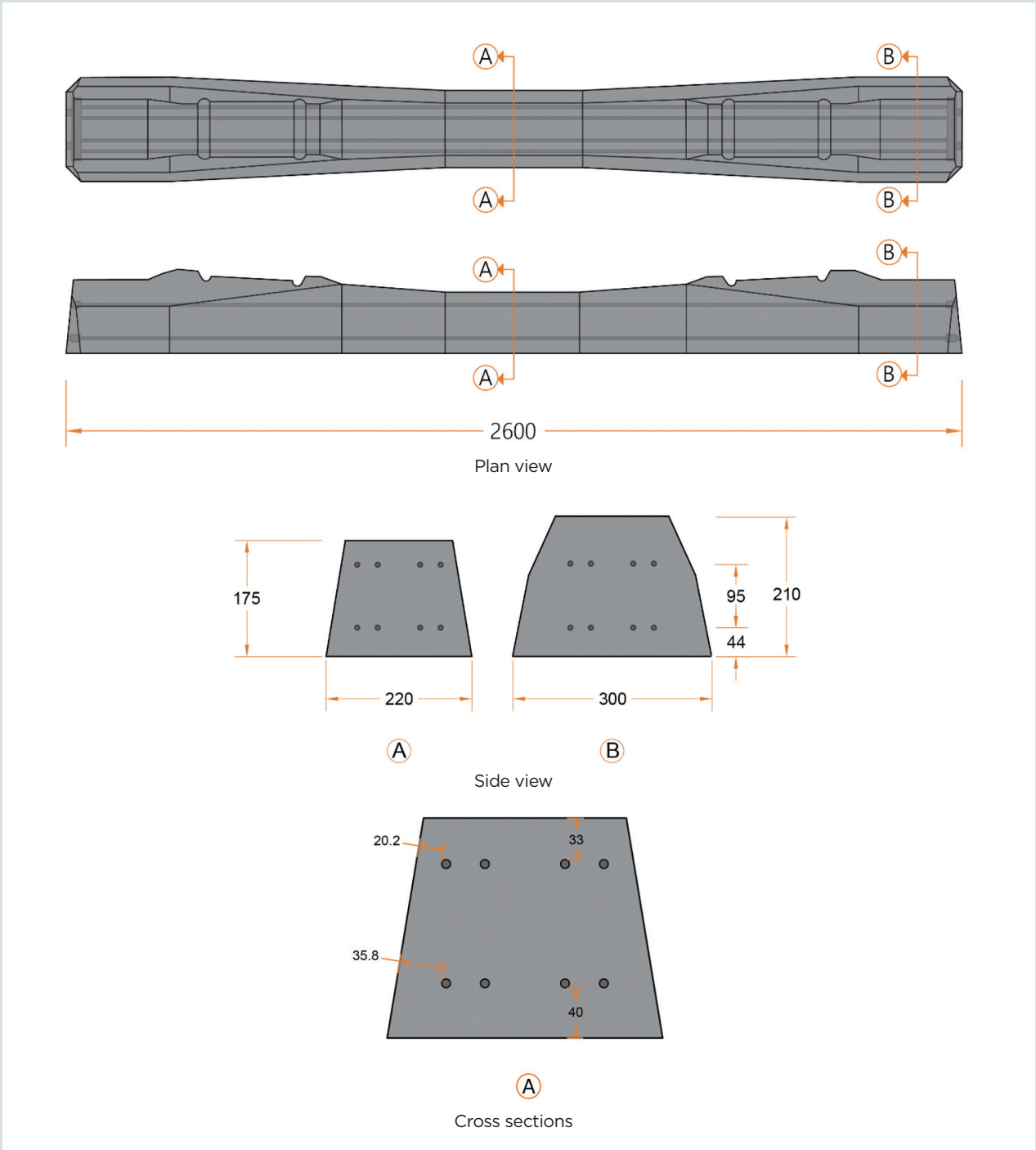

Figure 2. B70 concrete sleeper. Note: All dimensions are in mm. 1 mm = 0.0394 in.

Formation of longitudinal cracks in sleeper center adjacent to lower layer of wires

The next stage of deterioration is the appearance of cracks near the lower layer of reinforcing wires in the center of the sleeper. **Figure A.5** shows that these cracks emerge longitudinally at both lateral surfaces of the sleeper.

Extension of cracks to both ends of sleeper and failure

The longitudinal cracks spread rapidly due to the passing loads. As a result, more irregularly shaped cracks emerge. This irregularity is due to the different environmental conditions of sleepers and train loading. Extension of longitudinal cracks to both ends of the sleepers and formation of cracks in

other directions and along other surfaces leads to the failure of concrete sleepers. Most of the sleepers observed in the field were at this third stage, indicating that the failure process was relatively rapid (**Fig. A.6**).

Analytical basics of the chloride diffusion model in concrete sleepers

Corrosion due to chloride in concrete begins with the elimination of the protective layer around the reinforcing steel. For this phenomenon to occur, the chloride concentration in the concrete should exceed a certain amount, which is called the critical chloride content.[21] Therefore, to predict the onset of corrosion, chloride diffusion in concrete should be modeled mathematically. For unsteady conditions, Fick's second law is commonly used to express the diffusion of matter due to a concentration difference in three dimensions of x, y, and z versus time t:[22]

$$\frac{\partial C}{\partial t} = \frac{\partial}{\partial x}\left(D\frac{\partial C}{\partial x}\right) + \frac{\partial}{\partial y}\left(D\frac{\partial C}{\partial y}\right) + \frac{\partial}{\partial z}\left(D\frac{\partial C}{\partial z}\right) \quad (1)$$

where

C = concentration of matter

x = location along the x axis

D = diffusion rate of matter

y = location along the y axis

z = location along the z axis

The diffusion rate varies with many factors, such as time and temperature. By placing surface chloride as the boundary condition and initial chloride as the initial condition in Eq. (1), this differential equation can be written as follows:[22]

$$C_{(x,t)} = c_s - \left(c_s - c_i\right) erf\left(\frac{x}{\sqrt{4Dt}}\right) \quad (2)$$

where

c_s = surface chloride concentration

c_i = initial chloride concentration

In addition, the diffusion rate D, or more specifically in this case, the diffusion coefficient of chloride in concrete, is not constant and depends on time and environmental conditions. Many models have been proposed to explain the effect of these conditions on the diffusion coefficient. One of the most famous models expresses the effect of time on the diffusion coefficient as follows:

$$D = D_0\left(\frac{t_0}{t}\right)^m \quad (3)$$

where

D_0 = initial diffusion rate

t_0 = time at which D_0 is measured

m = aging coefficient

The aging coefficient m is a constant coefficient related to the mixing condition and mixing proportions obtained from the results of experiments on different ages of concrete.[23,24]

After determining the aging coefficient, the amount of chloride at the steel wire surface should be determined and compared with the critical chloride content to calculate the corrosion initiation time. As soon as the amount of chloride at the steel wire surface exceeds the critical chloride content, the steel wire's corrosion process begins. Because, in this model, the critical chloride content is considered to be the determining criterion for corrosion initiation, this value becomes more important in predicting the corrosion time. Many researchers have investigated the critical chloride content and its measurement method. Because various factors, such as the surface conditions of steel wires, surface contact of steel wire and concrete, the half-cell potential of steel wires, concrete properties, cement and admixture properties, moisture, temperature, and pH affect the critical chloride content, a specific amount that is applicable for all structures and, consequently, for all prediction models cannot be determined. Due to the variety of influencing factors, a wide range of critical chloride content in structures, from 0.1% to 1.96% of binder weight, has been reported.[25] Prominent cement and concrete specifications list the allowable amount of initial chloride content for prestressed concrete. EN 13230, which includes specifications for prestressed concrete sleepers, does not specify the amount of allowable initial chloride.[26] ACI 222 specifies an allowable acid-soluble chloride content of 0.08% by weight of cement, and EN 206 has a maximum total chloride content of 0.1% to 0.2% by weight of cement.[27,28]

The development and completion of the chloride diffusion model, as mentioned earlier, requires the results of experimental tests. Therefore, all factors of the model proposed in this study are extracted from the experimental results. Surface chloride content c_s, initial chloride content c_i, critical chloride content c_{cr}, and the chloride diffusion coefficient D were determined for desert conditions from concrete sleeper tests and the amount of diffusion coefficient at early ages. The values were obtained from cubic samples that are described in the following sections.

Laboratory and field studies

Sampling from on-site sleepers

Samples were collected from cracked concrete sleepers to obtain the chloride profile in the Rudshur-to-Shur-e Gaz block on the Bam-to-Zahedan line. Torres-Luque et al. notes that there are different methods to determine the chloride content within concrete elements, and they can be divided into field and labora-

tory tests.[29] Because the chloride measurements were to be performed both in the laboratory and the field, the Volhard method (powdering) was selected to investigate chloride content as the primary approach in this study. Accordingly, powder samples were taken from three cracked concrete sleepers at three points with equal distances and six depths each, according to ASTM C1152[30] and ASTM C42[31] (**Fig. 3**). These specimens were taken from the midspan and shoulder section of sleepers (**Fig. 4**).

After performing the acid-soluble chloride test on powder samples obtained from the line, two concrete sleepers were selected and transferred to the laboratory to access all sides of the element, achieve higher accuracy in sampling, and carry out nondestructive tests. Attempts were made to select sleepers that were in the first stage of the deterioration process and were suitable for shipment and nondestructive testing to illustrate the initial cracking patterns.

The midspan of the sleepers was perceived to be the critical section for cracking. Therefore, the laboratory sampling was limited to the sleeper's midspan. Drilling was performed on the lateral and bottom surfaces at the midspan (**Fig. 5**), and grinding at eight depths was accomplished according to ASTM C1152[30] and ASTM C42.[31] Because there was efflorescence on the surface of the sleepers and the surface concrete probably contained a high amount of salt, the first 1 mm (0.04 in.) of powder was removed and the acid-soluble chloride test was not performed on that depth.

Figure 3. Sampling from deteriorated concrete sleepers.

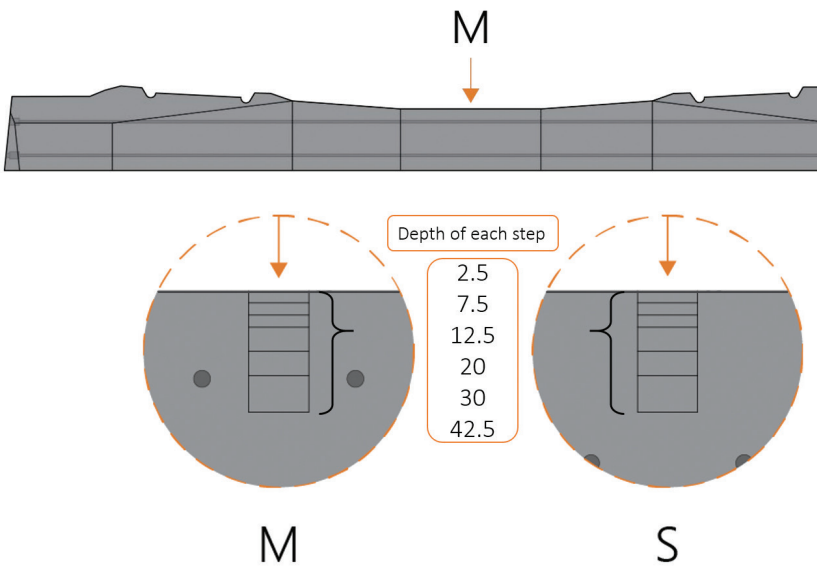

Figure 4. Sampling sections on concrete sleepers. Note: All dimensions are in millimeters. M = midspan; S = shoulder. 1 mm = 0.0394 in.

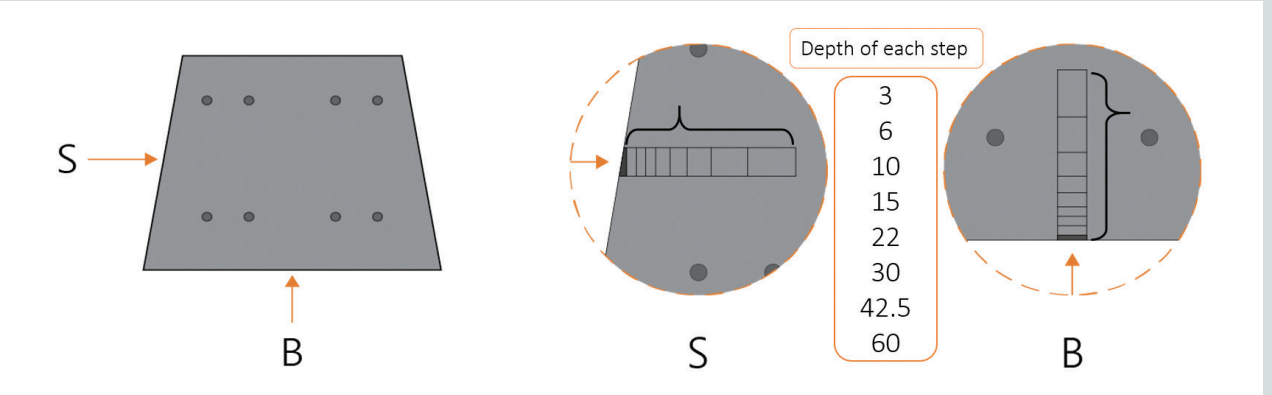

Figure 5. Sampling from the bottom and the side surface of the concrete sleeper. Note: All dimensions are in millimeters. B = bottom; S = side. 1 mm = 0.0394 in.

Determination of half-cell potential and rate of corrosion

To determine the potential and corrosion onset time, equipment based on the galvanostatic pulse method was used as a fast and nondestructive in-place and lab polarization method. In this method, based on ASTM C876,[32] the electrode (here silver/silver chloride [Ag/AgCl]) is placed on the concrete surface and a voltmeter measures the potential difference between the electrode and the wire. In this study, an electricity flow of 40 to 100 µA and a 10-second pulse were applied to the concrete by a probe. By receiving the reflection of this pulse by the device, the corrosion rate, single-electrode electrical resistance, polarized electrical resistance, and half-cell potential of the corrosion cell can be measured and calculated. **Figure 6** shows the test sections and the electrode connection junction. Because the wire of the upper layer of reinforcement and near the surface was predicted to be more critical in terms of corrosion severity, the half-cell potential test was performed by connecting the device electrode to this wire.

Sampling from laboratory cube samples

Cubic samples were made to determine the chloride diffusion coefficient at early ages in concrete. Several cubic samples in 150 × 150 × 150 mm (6 × 6 × 6 in.) molds were cast (**Fig. A.7**). To obtain maximum similarity between these specimens and the prestressed concrete sleepers, the following mixture proportions were used: 0.32 water-cement ratio, cement content of 450 kg/m^3 (760 lb/yd^3), gravel and crushed aggregate of the best quality and without any contamination with a maximum dimension of 19 mm (0.75 in.), and no additives. One-day accelerated curing was then carried out according to Iranian National Standard No. 21498.[33]

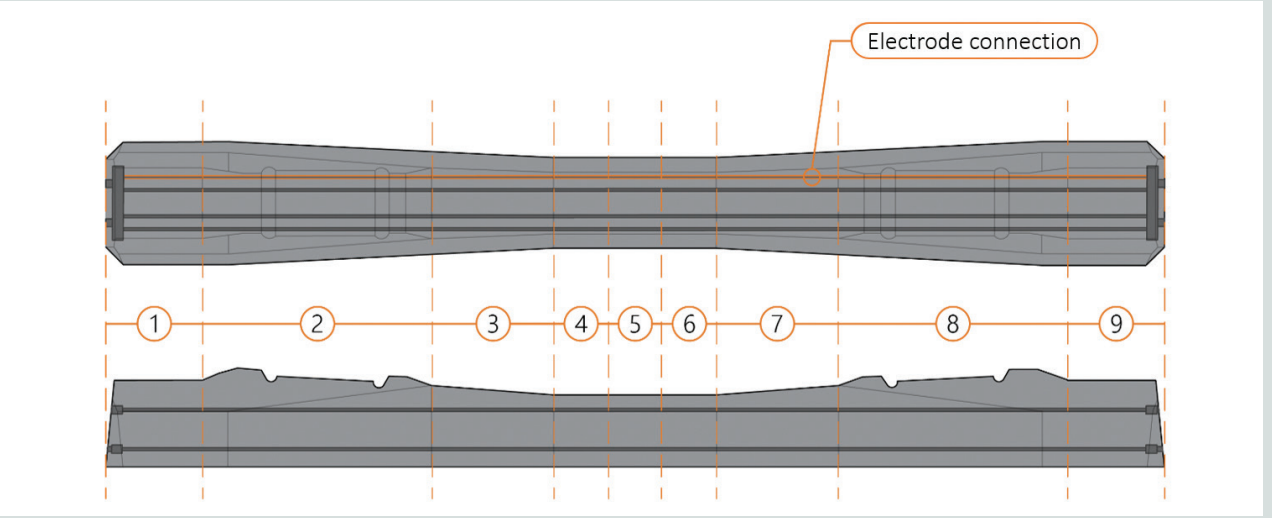

Figure 6. Sections of corrosion rate test and half-cell potential test and electrode connection to steel wire.

After the concrete curing period, the compressive strength test was conducted and a mean compressive strength of 47.25 MPa (6.85 ksi) was recorded from cubic samples as proof of similarity between the concrete in sleepers and cubic samples, according to Iranian National Standard no. 21498[33] and EN 13230.[26] Then, the specimens were immersed in a sodium chloride solution in accordance with ASTM C1556.[34] After the molds were opened and the specimens were dried in the open air, all of the specimens' surfaces except the finished one were sealed entirely with a two-component epoxy. After the epoxy coating was dried, the samples were placed in a 165 g/L (1.38 lb/gal.) sodium chloride (NaCl) solution at 26°C (79°F). Ninety days afterward, the samples were removed from the solution and the surface of the concrete was prepared for testing. It is noteworthy that, according to ASTM C1556, the minimum time for immersion should be 35 days; however, for concrete with low water-cement ratios, it is suggested that the immersion time be extended. Due to the recommendation of ASTM C1556, almost triple the minimum immersion time (90 days) was used for this testing. Grinding was subsequently carried out on eight depths according to ASTM C1556, and the first 2 mm (0.08 in.) of powder was discarded because it could have affected the profile due to high salt levels. According to the standard, this experiment was the shortest simulation of long-term exposure of chloride ions to concrete sleepers.

Determination of chloride profile and diffusion coefficient

An acid-soluble chloride test was performed by titration based on ASTM C1152[30] on powder samples from site sleepers, sleepers transferred to the laboratory, and cubic samples. The principal difference between the acid-soluble chloride test and the water-soluble chloride test is that the acid-soluble chloride test releases the bound chloride ion and measures it. Therefore, the amount of chloride measured in this experiment is more than the water-soluble chloride test and shows total chloride, including bound chloride and free chloride. After determining the percentage of chloride ions in each sample using Eq. (2) and fitting the modified results of the experiment (with the convection zone and inconsistent points removed), the values of D and c_s were obtained based on ASTM C1556[34] (**Fig. A.8** and **A.9**).

Calibration of the diffusion model

The chloride diffusion coefficient and surface chloride content were obtained by fitting the chloride-ion profiles to Eq. (2). Because the sleepers on the site were sampled from two sections (midspan and shoulder), their naming convention is based on the first letters of *shoulder* (S) and *midspan* (M). The number before the letter indicates the sleeper's number. Samples taken from the sleepers transferred to the laboratory are named based on the surface that was sampled. For the side surface, S is used, and for the bottom surface, B is used. The number after the letter also corresponds to the sleeper number.

Samples were taken from the top surface where the wire depth was 33 mm (1.3 in.) for the midspan section and 60 mm (2.4 in.) for the shoulder section (**Fig. 2**). Results showed that the chloride content exceeded the critical chloride content in all samples, predicting the corrosion at these sections.

Table 1 summarizes the results of the chloride profiles for the field sleepers and shows that the diffusion coefficient values vary greatly, ranging from 1.67 to 7.10 × 10^{-12} m^2/sec (1.80 to 7.55 × 10^{-11} ft^2/sec). This wide range is probably due to the low sampling depths and sampling error at the site. For this reason, two cracked concrete sleepers were transported to the laboratory to be sampled in chloride-exposed sections.

Table 2 shows the results of the acid-soluble chloride test performed on the sleepers transported to the laboratory. The chloride diffusion coefficients in these experiments (Table 2) had values ranging from 3.48 to 4.04 × 10^{-12} m^2/sec (3.75 to 4.35 × 10^{-11} ft^2/sec), which is a relatively narrower range

Table 1. Results from chloride profiles for field sleepers

	1S	1M	2S	2M	3S	3M	Average
Chloride diffusion coefficient, × 10^{-12} m^2/sec	4.41	2.38	3.27	1.23	7.01	1.67	3.63
Surface chloride content, % by weight of concrete	0.34	0.14	0.52	0.42	0.23	0.35	0.33

Note: 1S = shoulder sample 1; 1M = midspan sample 1; 2S = shoulder sample 2; 2M = midspan sample 2; 3S = shoulder sample 3; 3M = midspan sample 3. 1 m^2/sec = 10.764 ft^2/sec.

Table 2. Results of chloride profiles for sleepers transported to the laboratory

	Sleeper 1		Sleeper 2		Average
	S1	B1	S2	B2	
Chloride diffusion coefficient, × 10^{-12} m^2/sec	4.04	3.49	3.61	3.48	3.77
Surface chloride content, % by weight of concrete	0.21	0.32	0.21	0.33	0.27

Note: B1 = sleeper 1 bottom sample; B2 = sleeper 2 bottom sample; S1 = sleeper 1 side sample; S2 = sleeper 2 side sample. 1 m^2/sec = 10.764 ft^2/sec.

than in the previous tests on field samples. As expected, the chloride diffusion coefficients were similar, probably due to the selection of sleepers for a single block and with similar mixture proportions. Discarding the initial 2 mm (0.08 in.) of powder and sampling at eight depths had a positive impact on the increased accuracy of the results. Another data point collected was the amount of surface chloride in the profile. Table 2 shows that the surface chloride in the bottom surfaces (0.32% and 0.33%) was higher than in the side surfaces (0.21%), indicating relatively worse environmental conditions on the bottom of the sleepers.

For transferred sleepers, which were sampled from the side surface and the bottom surface, the corresponding steel wire depths (Fig. 2) were 21.5 and 35.8 mm (0.85 and 1.41 in.), respectively.

As with the sleepers on-site, the chloride content at the wire depth exceeded the critical chloride content in these samples, indicating the onset of corrosion in the sleeper.

For these sleepers, the initial chloride content was obtained by an in-depth sampling of the two sleepers, 0.013% and 0.015% by weight of concrete for sleepers 1 and 2. The initial chloride content limits specified in ACI 222 and EN 206 are 0.016% and 0.020%, respectively. The specified values are given in percentages by cement weight, multiplied by 0.2, and with a binder content of 450 kg/m^3 (760 lb/yd^3). The initial chloride contents in the two sleepers were within the allowable range of the listed specifications.

Figure A.10 shows the results of the half-cell potential test on the concrete sleepers transferred to the laboratory. According to half-cell potential instruction, if the half-cell potential range varies from -350 to -500 mV, the probability of corrosion in the reinforcement is 95%. With this in mind, in all sections except for sections 1, 2, 8, and 9 of sleeper 1 and section 1 of sleeper 2, corrosion has started at a 95% probability. This figure also shows that the half-cell potential in the midspan of the sleeper has lower values than the shoulder and rail seat, indicating the progression of corrosion in the midspan relative to the sides.

For sleeper 1, the first sections exceeding -350 mV potential were sections 3 and 7. Assuming this value of potential as the most probable corrosion initiation point, these two sections were used to determine critical chloride contents. Therefore, concrete powder sampling was performed in the area between the steel wires at sections 3 and 7. The results of the acid-soluble chloride test for sections 7 and 3 gave chloride contents of 0.067% and 0.069% by concrete weight, respectively, with an average of 0.068%. The average value was used as the critical chloride content, where corrosion is highly expected to begin.

Table 3 compares the critical chloride content in the present study with other studies.[35–38] As mentioned previously, many factors affect the critical chloride content.[25] Table 3 shows the different values obtained for critical chloride content in multiple studies; however, the amount measured in the present experiment is in line with the results of other investigations.

After the accelerated curing period, compressive strength tests were performed on cubic specimens. The compressive strength of these specimens, with an average of 47.25 MPa (6.85 ksi), which is greater than 45 MPa (6.5 ksi), met the criteria for accepting concrete sleepers after the accelerated curing (sample 1 was 48 MPa [7.0 ksi] and sample 2 was 46.5 MPa [6.74 ksi]).

Table 4 shows the chloride diffusion coefficients and surface chloride contents for the cubic samples. As expected, the chlo-

Table 3. Comparison of critical chloride content values from multiple studies

Description of sample	Critical chloride content, % by weight of concrete	Source
Concrete sleepers from the Iranian desert	0.068	This study
Persian Gulf	0.05	Shekarchi et al. (2008)
Concrete containing 0% to 35% fly ash	0.07	Chalee et al. (2009)
Concrete containing 0% to 35% fly ash	0.028 to 0.041	Cheung and Kyle (1996)
A pier in the Persian Gulf	0.073	Shekarchi et al. (2011)
Normal concrete	0.06	Lambert et al. (1991)

Table 4. Values of the chloride diffusion coefficient and amount of surface chloride in samples immersed for 90 days

	Sample 1	Sample 2	Average
Chloride diffusion coefficient, × 10^{-12} m^2/sec	7.54	7.80	7.62
Surface chloride content, % by weight of concrete	0.90	0.94	0.92

Note: 1 m^2/sec = 10.764 ft^2/sec.

ride diffusion coefficient in 90-day samples was much higher than the diffusion coefficient of concrete sleepers, which is due to the growth of hydration and maturation of concrete. Surface chloride content was also high owing to accelerated conditions. To model the change of the diffusion coefficient over time, Eq. (3) was used. Substituting the diffusion coefficient D from Table 2 (which is also more accurate) and the diffusion coefficient at early ages D_0 from Table 4 into Eq. (3), the aging coefficient can be calculated as 0.2, which is approximately equal to the aging coefficient in the ACI Life 365 model.[10]

In Eq. (2), if c_{cr} is used as the corrosion threshold content on the left side of the equation and the equation is solved for t, Eq. (4) will be the equation for the location of points on the concrete cross section over time that have reached the corrosion threshold, and corrosion will initiate in those areas if reinforcement is present.

$$x = erf^{-1}\left(\frac{c_s - c_{cr}}{c_s - c_i}\right)\sqrt{4Dt} \tag{4}$$

where

erf^{-1} = inverse of the error function or erf

Now, by assigning a surface chloride content c_s of 0.27, a critical chloride content c_{cr} of 0.068, an initial chloride content c_i of 0.014, and a chloride diffusion coefficient D of $7.622\left(\frac{0.25}{t}\right)^m$ and simplifying, Eq. (4) can be rewritten as follows:

$$x_s = 1.76\sqrt{181.88 t_s^{0.8}} \tag{5}$$

where

t_s = time of corrosion initiation in sleeper wires

x_s = concrete cover of sleeper wires

Figure 7 is the graph of Eq. (5) and shows the points that have reached the onset of the corrosion stage over time. In order to better illustrate the corrosion initiation at the concrete sleeper section, Fig. 7 shows the concrete cover (the distance between the concrete surface and the nearest steel surface) at the critical cross section (midspan) of the B70 concrete sleeper (Fig. 2). It can be observed that at the midspan of the sleeper, for the first reinforcement in the upper layer, corrosion has a rapid onset and reaches the corrosion initiation stage at about 8.5 months. It is worth noting that this value has been confirmed according to the maintenance reports and field inspections of the maintenance team in charge of the critical blocks in the Shur-e Gaz area.

Sensitivity analyses on the model parameters

A parametrical study was conducted to investigate the sensitivity of model results to the variation of contributing parameters. It is clear that in other studies, the role of each parameter introduced in this paper has been explored; however, in

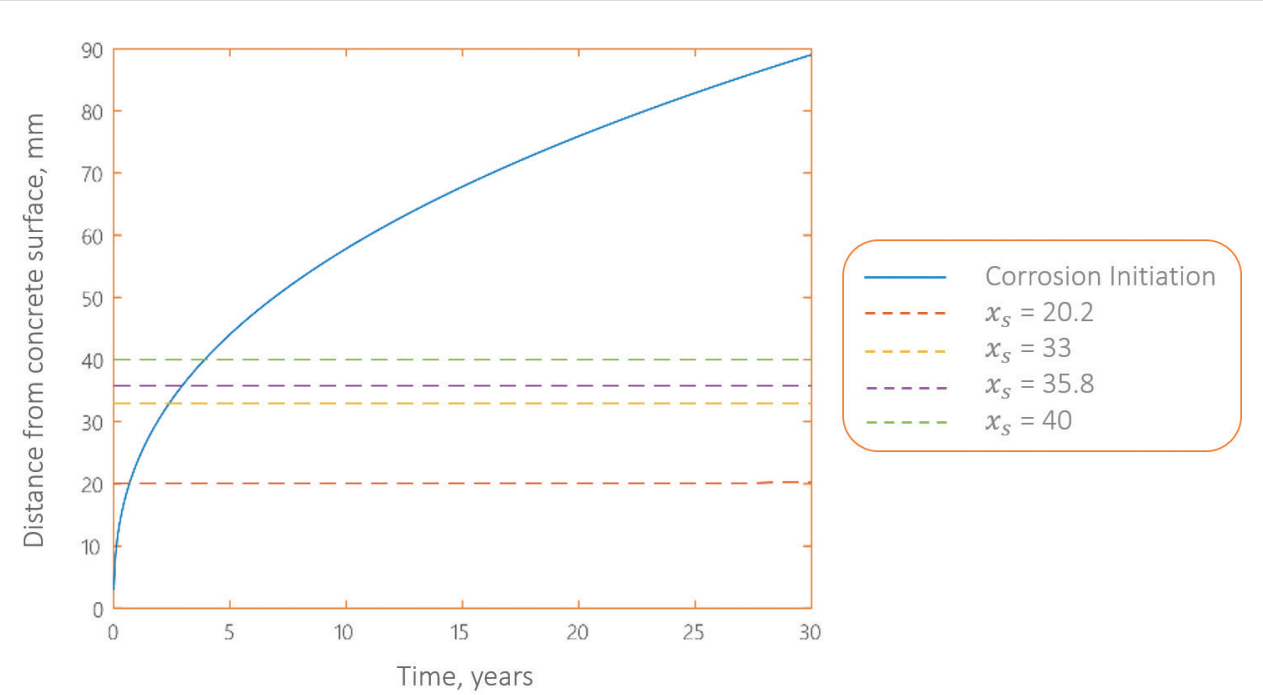

Figure 7. Corrosion prediction graph based on the developed model. Note: x = distance from the concrete surface. 1 mm = 0.0394 in.

order to give a practical sense for engineers and inspectors, there is a need to evaluate important parameters. The influential factors on the chloride diffusion model, including initial chloride content c_i, surface chloride content c_s, chloride diffusion coefficient D, and distance from the concrete surface x_s, were examined.

The initial chloride content of the sleepers is within the permissible limit. Also, the initial chloride content in cubic samples was measured to be about 0.017% by weight of concrete, which is approximately equal to the specified limit in ACI 222. Therefore, it may not be conceivable to reduce the amount of initial chloride content. However, the corrosion initiation curve for the values of 0.005%, 0.01%, 0.014%, and 0.02% were considered in **Fig. 8**. Decreasing the initial chloride content from 0.014% to 0.005% resulted in a slight decrease in the corrosion initiation time, especially for the 20.2 mm (0.80 in.) concrete cover.

Surface chloride content mainly varies with environmental conditions, such as salt concentration, moisture content, and concrete properties. This amount ranged from 0.14% to 0.50% due to the different conditions of each sleeper. It was also observed that this amount was higher beneath the sleeper than on the lateral surface. **Figure 9** shows the effect of surface chloride content in the range of 0.10% to 0.60% on corrosion initiation time.

According to Fig. 9, corrosion initiates much later at low percentages of surface chloride content. For example, with 0.10% chloride content, for the nearest steel wire, corrosion begins about eight years after exposure. Because surface chloride is highly dependent on environmental conditions, it is not in the user's control, so it would not be an appropriate solution to reduce surface chloride content to improve the durability of concrete sleepers in desert areas.

The chloride diffusion coefficient in the site sleepers ranged from 1.67 to 7.10 × 10^{-12} m^2/sec (1.80 to 7.64 × 10^{-11} ft^2/sec). On average, these coefficients have been measured for site sleepers as 3.36 × 10^{-12} m^2/sec (3.62 × 10^{-11} ft^2/sec) and sleepers transported to the laboratory as 3.77 × 10^{-12} m^2/sec (4.06 × 10^{-11} ft^2/sec). **Figure 10** shows the effect of diffusion coefficients of 0.5, 1.5, 2.5, 3.5, and 4.5 × 10^{-12} m^2/sec (0.54, 1.6, 2.7, 3.8, and 4.8 × 10^{-11} ft^2/sec) on the corrosion initiation time.

Low values of the diffusion coefficient have a significant impact on delaying the onset of corrosion. For example, corrosion starts at a diffusion coefficient of 0.5 × 10^{-12} m^2/sec (0.54 × 10^{-11} ft^2/sec) for concrete cover of 20.2 mm (0.80 in.) after six years, and at a diffusion coefficient of 1.5 × 10^{-12} m^2/sec (1.6 × 10^{-11} ft^2/sec) for concrete cover of 33 mm (1.3 in.) after 6.5 years.

The concrete cover is an essential factor affecting the time of corrosion initiation, and sensitivity analysis of this parameter can give valuable information to engineers for modifying the design criteria. In the concrete sleepers in desert areas, cracking started from the midspan at the upper

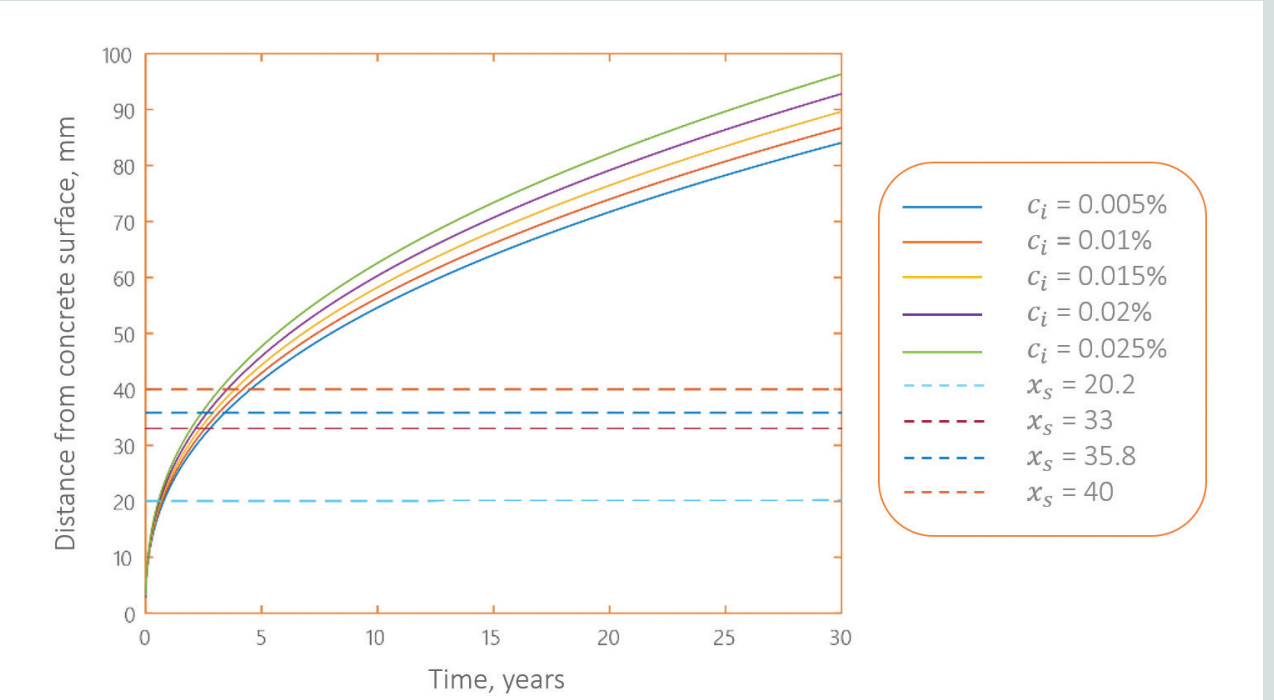

Figure 8. Influence of initial chloride content on corrosion initiation. Note: c_i = initial chloride concentration; x = distance from the concrete surface. 1 mm = 0.0394 in.

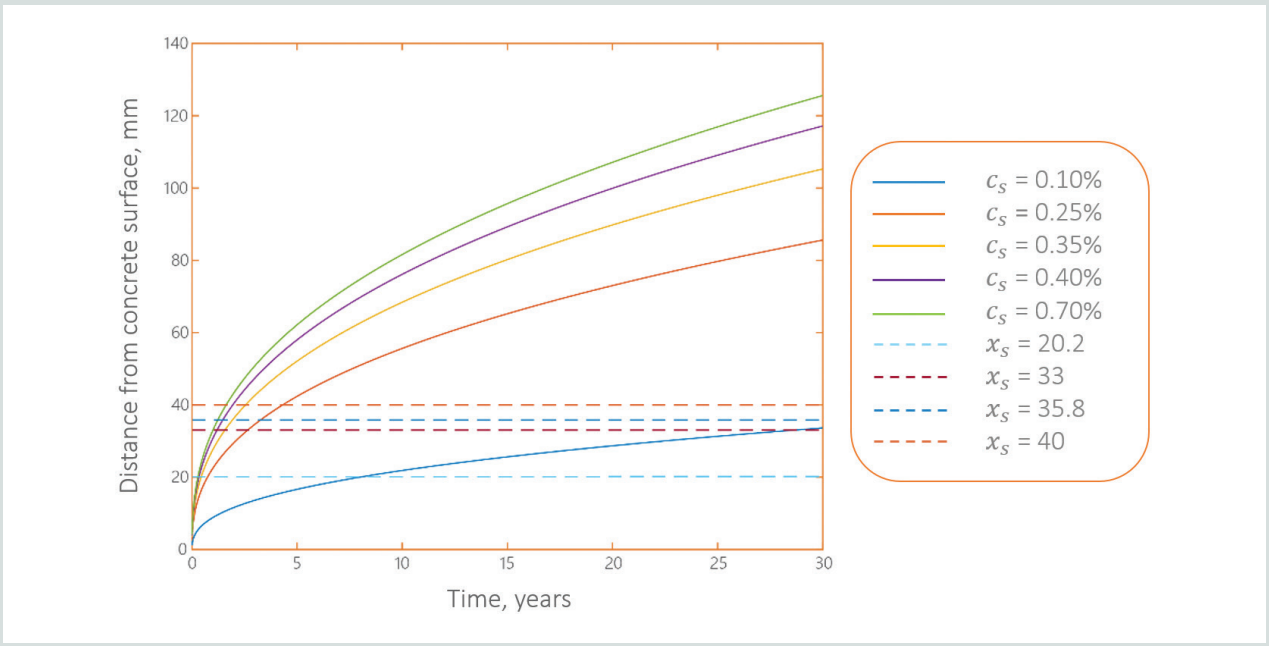

Figure 9. Influence of surface chloride content on corrosion initiation. Note: c_i = initial chloride concentration; c_s = surface chloride concentration; x = distance from the concrete surface. 1 mm = 0.0394 in.

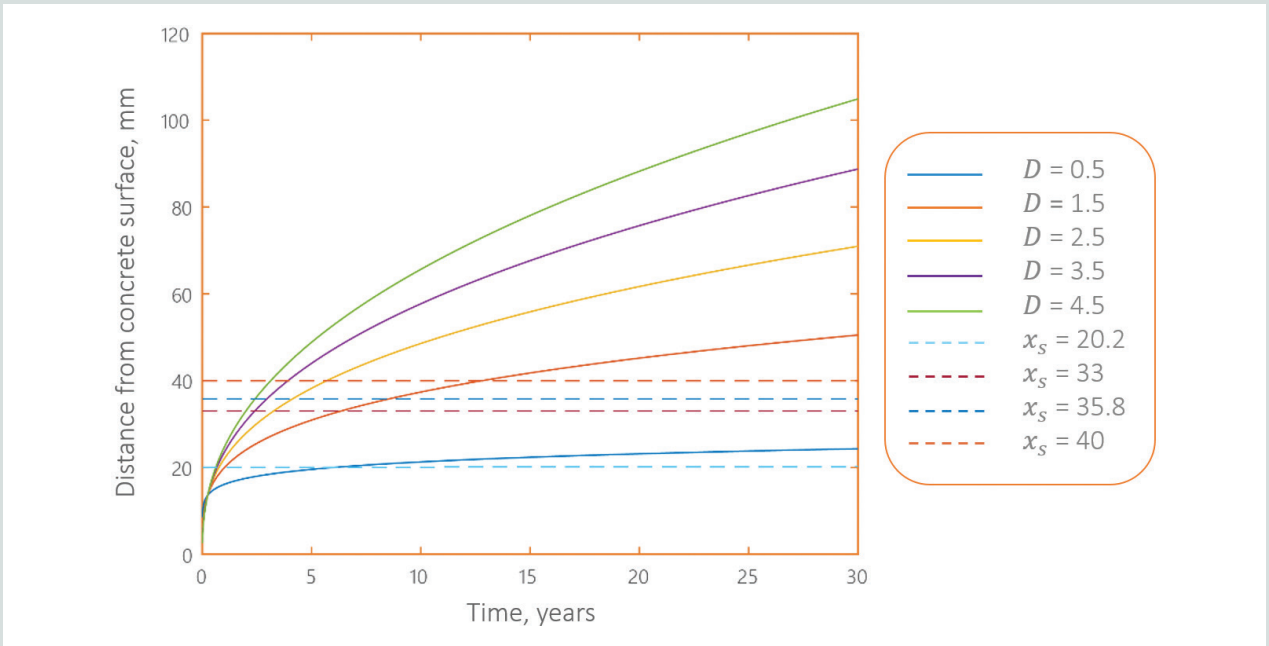

Figure 10. Influence of chloride diffusion coefficient on corrosion initiation. Note: D = diffusion coefficient; x = distance from the concrete surface. 1 mm = 0.0394 in.

layer of reinforcement and extended to the sides. From Fig. 2, it can be observed that this is due to the low concrete cover (20.2 mm [0.80 in.]) in the upper layer for the first steel wire. **Figure 11** shows the effect of different cover values from 20 to 40 mm (0.8 to 1.6 in.) on the time of corrosion initiation.

Figure 11 shows that increasing concrete cover has a meaningful impact on deferring corrosion. With only a 10 mm (0.4 in.) increase in concrete cover from 20 to 30 mm (0.8

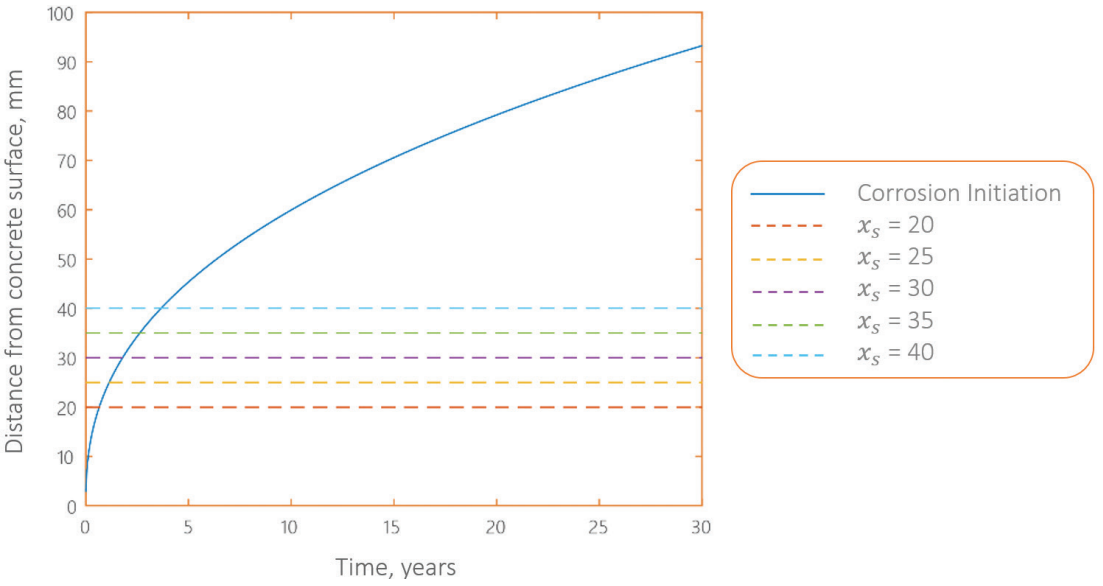

Figure 11. Influence of concrete cover on corrosion initiation. Note: x = distance from the concrete surface. 1 mm = 0.0394 in.

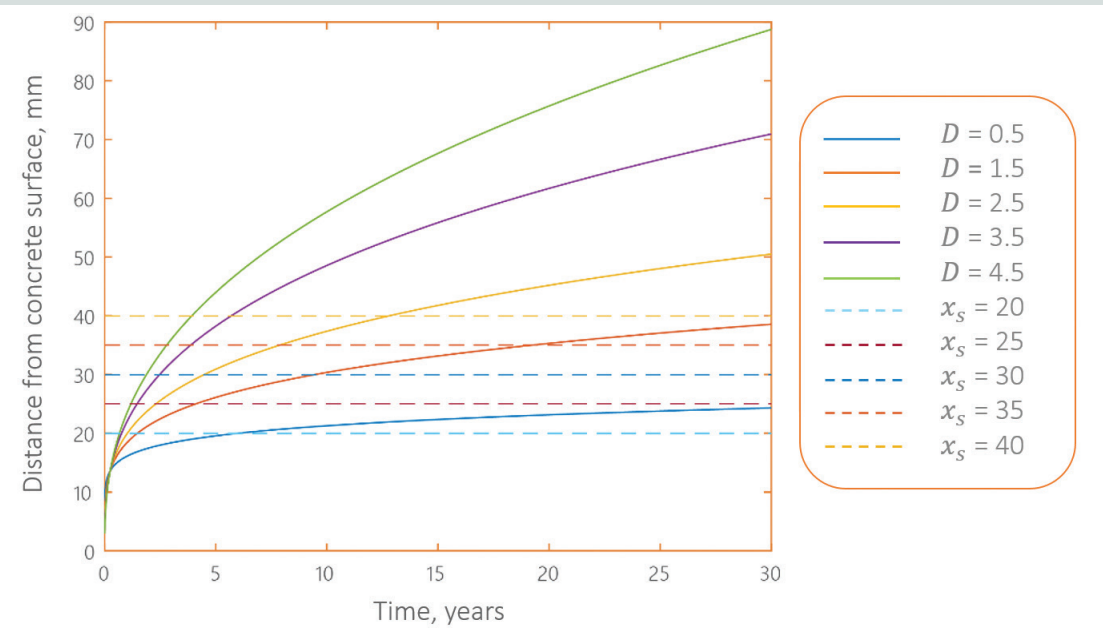

Figure 12. The effect of increasing concrete cover and decreasing diffusion coefficient on corrosion initiation time. Note: D = diffusion coefficient; x = distance from the concrete surface. 1 mm = 0.0394 in.

to 1.2 in.), the corrosion initiation is delayed by more than one year.

Obviously, according to Fig. 11, increasing the concrete cover alone is not sufficient to improve the durability of concrete sleepers in desert areas. Increased concrete cover, if combined with a reduced chloride diffusion coefficient, can have a significant impact on improving the durability of concrete sleepers. To better understand the issue, the simultaneous effect of increasing concrete cover and reducing the diffusion coefficient on the corrosion initiation time is presented in **Fig. 12**. It can be clearly seen in this graph that in order to

obtain sufficient delay in corrosion initiation, both the reduction of the chloride diffusion coefficient and the increase of concrete cover are required.

Conclusion

This research investigated the chloride diffusion in concrete sleepers in desert areas and proposed a model to explain and predict the time of corrosion initiation. The model was developed based on the empirical data obtained from concrete sleepers in desert areas and will be valid under these circumstances. The results of this study can be used to modify concrete sleepers to improve their resistance to the environmental conditions of Iranian deserts.

The findings of the present research can be summarized as follows:

- The cause of early and immediate cracking of concrete sleepers in desert areas is the corrosion of prestressed wires due to chloride-ion penetration from the environment to the concrete structure.
- Cracking and deterioration in concrete begin due to prestressed wire deterioration from the upper layer in the midspan of the B70 concrete sleeper and extend to the ends.
- By developing the chloride diffusion model and applying the experimentally-obtained coefficients, it was found that corrosion at the most critical section and the nearest steel wire to the surface begins approximately 8.5 months after exposure.
- Decreasing the chloride diffusion coefficient has a significant effect on delaying corrosion initiation.
- By decreasing the diffusion coefficient from 3.5×10^{-12} m^2/sec (3.8×10^{-11} ft^2/sec) to 0.5×10^{-12} m^2/sec (0.54×10^{-11} ft^2/sec), the onset of corrosion is delayed from 8.5 months to about six years for the first steel wire, with a 20.2 mm (0.80 in.) concrete cover. This reduction can be achieved by modifying the mixture proportions and adding supplementary cementitious materials, such as silica fume.
- Increasing concrete cover is recognized as an essential factor affecting the time of corrosion initiation. Increasing concrete cover from 20 to 35 mm (0.8 to 1.4 in.) delays corrosion initiation from 8.5 months to 2 years 8.5 months. Although this factor alone is not sufficient, if combined with the reduction of the chloride diffusion coefficient, as a practical and reliable solution, it can improve the durability of concrete sleepers in terms of chloride-ion penetration and steel corrosion.

Acknowledgment

The authors appreciate the contributions of the General Directorate of Railway and Railway Structures, CBG Concrete Sleeper Plant, South East Railway and East Railway of Iran, and Mohammad Hosein Tadayon.

References

1. Kinsley, D. B. 1970. *A Geomorphological and Palaeoclimatological Study of the Playas of Iran, Part 1*. Reston, VA: Geological Survey, U.S. Department of the Interior.
2. Zakeri, J. A., M. Esmaeili, and M. Fathali. 2011. "Evaluation of Humped Slab Track Performance in Desert Railways." *Proceedings of the Institution of Mechanical Engineers, Part F: Journal of Rail and Rapid Transit* 225 (6): 566–573. https://doi.org/10.1177/0954409711403677.
3. Sadeghi, J. M., and A. Babaee. 2006. "Structural Optimization of B70 Railway Prestressed Concrete Sleepers." *Iranian Journal of Science and Technology Transaction B: Engineering* 30 (4): 461–473.
4. Van Dyk, B. J., M. S. Dersch, and J. R. Edwards. International Concrete Crosstie and Fastening System Survey 2012. Washington, DC: United States Department of Transportation, Federal Railroad Administration. https://railroads.dot.gov/sites/fra.dot.gov/files/fra_net/2878/RR_International%20Survey_CO20121217_CS20130201_final.pdf.
5. Bezgin, N. Ö. 2015. "Climate Effects on the Shoulder Width Measurements of Prestressed Concrete High Speed Railway Sleepers of Ballasted Tracks." *Measurement*, vol. 75: 201–209. https://doi.org/10.1016/j.measurement.2015.07.057.
6. Minoura, S., T. Watanabe, M. Sogabe, and K. Goto. 2017. "Analytical Study on Loading Capacity of Prestressed Concrete Sleeper." *Procedia Engineering*, vol. 199: 2482–2487. https://doi.org/10.1016/j.proeng.2017.09.409.
7. Moutassem, F., and I. Miqdadi. 2020. "Sustainability-Model Approach for Chloride Permeability Based on Concrete Mixture." *Structures*, vol. 28: 983–990. https://doi.org/10.1016/j.istruc.2020.09.041.
8. Kaewunruen, S., and A. M. Remennikov. 2009. "Progressive Failure of Prestressed Concrete Sleepers under Multiple High-Intensity Impact Loads." *Engineering Structures* 31: 2460–2473. https://doi.org/10.1016/j.engstruct.2009.06.002.
9. Shekarchi, M., P. Ghods, R. Alizadeh, M. Chini, and M. Hoseini. 2008. "DuraPGulf, a Local Service Life Model for the Durability of Concrete Structures in the South of Iran." *Arabian Journal for Science and Engineering* 33 (1): 77–88.

10. Ehlen, M. A. 2020. "Life-365 Service Life Prediction ModelTM Version 2.0." *Concrete International* 31 (5): 41–46. https://www.concrete.org/publications/internationalconcreteabstractsportal/m/details/id/56508.

11. Ashrafi, H. R., and A. A. Ramezanianpour. 2007. "Service Life Prediction of Silica Fum e Concretes." *International Journal of Civil Engineering* 5 (3): 182–197. http://ijce.iust.ac.ir/article-1-323-en.html.

12. *fib* (International Federation for Structural Concrete). 2006. *Model Code for Service Life Design*. *fib* Bulletin no. 34. Lausanne, Switzerland: *fib*. https://doi.org/10.35789/fib.BULL.0034.

13. Ramezanianpour, A., E. Jahangiri, B. Ahmadi, and F. Moodi. 2015 "Evaluation and Modification of *fib* Service Life Design Model for Persian Gulf Region." In *SP-303: Thirteenth International Conference on Advances in Concrete Technology and Sustainability Issues*, 337–354. Farmington Hills, MI: ACI (American Concrete Institute). https://doi.org/10.14359/51688145.

14. Siemes, A. J. M., and C. Edvardsen. 1999. "Duracrete: Service Life Design for Concrete Structures." In *Durability of Building Materials and Components 8. Service Life and Asset Management. Proceedings of the 8th International Conference on Durability of Building Materials and Components, 8dbmc, Volume 2: Durability of Building Assemblies and Methods of Service Life Prediction*, 1343–1356. Ottawa, ON, Canada: NRC Research Press.

15. Van der Wegen, G., R. B. Polder, and K. van Breugel. 2012. "Guideline for Service Life Design of Structural Concrete—A Performance Based Approach with Regard to Chloride Induced Corrosion." *Heron*, vol. 57: 153–168.

16. Mohammadzadeh, S., and E. Vahabi. 2011. "Time-Dependent Reliability Analysis of B70 Pre-stressed Concrete Sleeper Subject to Deterioration." *Engineering Failure Analysis* 18 (1):421–432.

17. Tadayon, M. 2016. *Investigating of the Causes of Damaged Sleepers in Sandy Desert Areas*. [In Persian.] Tehran, Iran: Iranian Railway Co.

18. Cooke, R. U., D. Brunsden, J. C. Doornkamp, and D. K. C. Jones. 1982. *Urban Geomorphology in Drylands*. Oxford, UK: Oxford University Press, on behalf of the United Nations University. https://doi.org/10.1002/esp.3290080617.

19. Walker, M. 2002. *Guide to the Construction of Reinforced Concrete in the Arabian Peninsula*. CIRIA (Construction Industry Research and Information Association)/The Concrete Society special publication vol. 577. Camberley, United Kingdom: CIRIA/The Concrete Society.

20. Amrolahi, A. 2017. *Statistics of Sandstone and Desert Areas of 2017*. [In Persian]. Tehran, Iran: General Directorate of the Islamic Republic of Iran Railways.

21. Mehta, P. K., and P. J. M. Monteiro. 2014. *Concrete: Microstructure, Properties, and Materials*. 4th ed. New York, NY: McGraw-Hill Education.

22. Basheer, L., J. Kropp, and D. J. Cleland. 2001. "Assessment of the Durability of Concrete from Its Permeation Properties: A Review." *Construction and Building Materials* 15 (2–3): 93–103.

23. Luping, T., and J. Gulikers. 2007. "On the Mathematics of Time-Dependent Apparent Chloride Diffusion Coefficient in Concrete." *Cement and Concrete Research* 37 (4): 589–595.

24. Mangat, P. S., and B. T. Molloy. 1994. "Prediction of Long Term Chloride Concentration in Concrete." *Materials and Structures*, vol. 27: 338–346. https://doi.org/10.1007/BF02473426.

25. Angst, U., B. Elsener, C. K. Larsen, and Ø. Vennesland. 2009. "Critical Chloride Content in Reinforced Concrete—A Review." *Cement and Concrete Research* 39 (12): 1122–1138.

26. BSI (British Standards Institution). 2016. *BS EN 13230—Railway Applications. Track. Concrete Sleepers and Bearers*. London, UK: BSI. https://doi.org/10.3403/BSEN13230.

27. ACI Committee 222. 2001. *Protection of Metals in Concrete Against Corrosion*. ACI 222R-01. Farmington Hills, MI: ACI.

28. BSI (British Standards Institution). *2013. BS EN 206—Concrete. Specification, Performance, Production and Conformity*. +A2:2021 incorporating corrigendum May 2014. London, UK: BSI.

29. Torres-Luque, M., E. Bastidas-Arteaga, F. Schoefs, M. Sánchez-Silva, and J. F. Osma. 2014. "Non-destructive Methods for Measuring Chloride Ingress into Concrete: State-of-the-Art and Future Challenges." *Construction and Building Materials*, vol. 68: 68–81. https://doi.org/10.1016/j.conbuildmat.2014.06.009.

30. ASTM Subcommittee C09.69. 2012. *Standard Test Method for Acid-Soluble Chloride in Mortar and Concrete*. ASTM C1152/C1152M-04(2012)e01. West Conshohocken, PA: ASTM International.

31. ASTM Subcommittee C09.61. 2020. *Standard Test Method for Obtaining and Testing Drilled Cores and Sawed Beams of Concrete*. ASTM C42/C42M-20. West Conshohocken, PA: ASTM International.

32. ASTM Subcommittee G01.14. 2015. *Standard Test Method for Corrosion Potentials of Uncoated Reinforcing Steel in Concrete*. ASTM C876-15. West Conshohocken, PA: ASTM International.

33. INSO (Iran National Standards Organization). 2017. *Railway Applications–Track—Concrete Sleepers and Bearers. Part 1: General Requirements*. Tehran, Iran: INSO.

34. ASTM Subcommittee C09.66. 2011. *Standard Test Method for Determining the Apparent Chloride Diffusion Coefficient of Cementitious Mixtures by Bulk Diffusion*. ASTM C1556-11a. West Conshohocken, PA: ASTM International.

35. Chalee, W., C. Jaturapitakkul, and P. Chindaprasirt. 2009. Predicting the Chloride Penetration of Fly Ash Concrete in Seawater. *Marine Structures* 22 (3): 341–353. https://doi.org/10.1016/j.marstruc.2008.12.001.

36. Cheung, M. S., and B. R. Kyle. 1996. "Service Life Prediction of Concrete Structures by Reliability Analysis." *Construction and Building Materials* 10 (1): 45–55. https://doi.org/10.1016/0950-0618(95)00055-0.

37. Shekarchi, M., F. Moradi-Marani, and F. Pargar. 2011. "Corrosion Damage of a Reinforced Concrete Jetty Structure in the Persian Gulf: A Case Study." *Structural and Infrastructure Engineering* 7 (9): 701–713. https://doi.org/10.1080/15732470902823903.

38. Lambert, P., C. L. Page, and P. R. W. Vassie. 1991. "Investigations of Reinforcement Corrosion. 2. Electrochemical Monitoring of Steel in Chloride-Contaminated Concrete." *Materials and Structures*, vol. 24: 351–358.

Notation

c_{cr} = critical chloride content

c_i = initial chloride concentration

c_s = surface chloride concentration

C = concentration of matter

D = diffusion rate of matter

D_0 = initial diffusion rate

m = aging coefficient

t = time at which the diffusion coefficient D is obtained

t_0 = time at which D_0 is measured

t_s = time of corrosion initiation in sleeper wires

x = location along the x axis

x_s = concrete cover of sleeper wires

y = location along the y axis

z = location along the z axis

About the authors

Morteza Esmaeili is a professor in the School of Railway Engineering at Iran University of Science and Technology in Tehran.

Sadegh Kaviani has an MSc in railway track engineering from the School of Railway Engineering at Iran University of Science and Technology.

Farzad Farivar is a PhD candidate in railway track engineering in the Institute of Railway Infrastructure Design at Graz University of Technology in Graz, Austria.

Abstract

There are approximately 600 km (370 mi) of railway passing through the desert areas in Iran. One of the important challenges associated with the degradation of railway structures in desert areas is chloride-ion invasion of the concrete, which causes the corrosion and swelling of bars, leading to the total destruction of concrete sleepers. Although numerous studies have been conducted on the prediction of bar corrosion in various reinforced concrete structures, there is no specific study on the prediction of bar corrosion in B70 concrete sleepers. This study investigates chloride diffusion in concrete sleepers and develops a prediction model using field and laboratory measurements. Sample profiles were taken from the Bam–Zahedan railway line for the determination of diffusion coefficients and initial and surface chloride contents. The early-age diffusion coefficient in concrete samples was obtained, and a prediction model was developed based on these parameters. Finally, a sensitivity analysis was performed in order to investigate the influential parameters on the initiation time of the corrosion. The results indicate that the effects of the chloride diffusion coefficient and the concrete cover were the leading factors in the corrosion initiation time.

Keywords

Chloride diffusion, concrete sleeper, corrosion, corrosion initiation prediction, desert area.

Review policy

This paper was reviewed in accordance with the Precast/Prestressed Concrete Institute's peer-review process. The Precast/Prestressed Concrete Institute is not responsible for statements made by authors of papers in *PCI Journal*. No payment is offered.

Publishing details

This paper appears in *PCI Journal* (ISSN 0887-9672) V. 68, No. 1, January–February 2023, and can be found at https://doi.org/10.15554/pcij68.1-02. *PCI Journal* is published bimonthly by the Precast/Prestressed Concrete Institute, 8770 W. Bryn Mawr Ave., Suite 1150, Chicago, IL 60631.

Reader comments

Please address any reader comments to *PCI Journal* editor-in-chief Tom Klemens at tklemens@pci.org or Precast/Prestressed Concrete Institute, c/o *PCI Journal*, 8770 W. Bryn Mawr Ave., Suite 1150, Chicago, IL 60631.